Predicting formation of self-organized patterns of cathodic spots in dc glow microdischarges in argon and helium

P. G. C. Almeida, M. S. Benilov, and M. J. Faria

Departamento de Física, Universidade da Madeira, Largo do Município, 9000 Funchal, Portugal

Modelling of high-pressure dc glow microdischarges in different gases is performed with the aim to explain why self-organized patterns have been observed in xenon but not in other gases such as argon. Modelling results show that conditions of argon microdischarges are indeed less favourable for the appearance of self-organization than the conditions of xenon microdischarges, which is due to lower cross sections of elastic collisions between electrons and atoms. It should be possible, however, to observe formation of self-organized patterns also in argon, and even in helium, provided that the pressure is sufficiently high and the microdischarge radius is large enough.

1. Introduction

Self-organized patterns of cathode spots have been observed in DC glow microdischarges in xenon, e.g., [1]. The patterns comprise two or more cathode spots and seem to appear at the transition from the normal mode to the abnormal mode.

The first steps towards a self-consistent modelling of these patterns were taken in [2-4]: modelling of microdischarges in xenon has revealed existence of multiple solutions for the same value of discharge current, some of the solutions describing normal discharge, others describing 2D (axially symmetric) patterns of cathodic spots, and others describing 3D patterns similar to those observed in the experiment [1].

A very interesting question is why modes with self-organized patterns have been observed in DC glow microdischarges in xenon but not in other gases such as argon [6]. In this work, calculations of microdischarges in different plasma-producing gases are reported. An explanation as to why self-organized patterns were not observed in argon microdischarges is proposed. It is predicted that self-organized patterns can, in principle, be observed in plasma-producing gases other than xenon provided that conditions are right.

2. The model

The plasma-producing gases considered in this work are argon and helium. The modelling of argon microdischarges has been performed in the framework of the basic model of glow discharge and in the framework of a more detailed model. The modelling of helium microdischarges has been performed in the framework of the basic model only. The basic model comprises equations of conservation of a single ion species (molecular ions) and the electrons, transport equations for the ions and the electrons written in the drift-diffusion local-field approximation, and the Poisson equation:

$$\nabla\cdot\mathbf{J}_i = w, \quad \mathbf{J}_i = -D_i\nabla n_i - \mu_i n_i \nabla\varphi,$$

$$\nabla\cdot\mathbf{J}_e = w, \quad \mathbf{J}_e = -D_e\nabla n_e + \mu_e n_e \nabla\varphi,$$

$$\varepsilon_0\nabla^2\varphi = -e(n_i - n_e),$$

where

$$w = n_e\alpha\mu_e E - \beta n_e n_i .$$

Here n_i, n_e, J_i, J_e, D_i, D_e, μ_i, and μ_e are number densities, densities of transport fluxes, diffusion coefficients, and mobilities of the ions and electrons, respectively; α is Townsend's ionization coefficient; β is the coefficient of dissociative recombination; φ is electric potential; $E = |\nabla\varphi|$ is the electric field strength; ε_0 is the permittivity of free space; e is the elementary charge.

The Townsend ionization coefficient was evaluated by means of formula:

$$\alpha = Cp\exp\left[-D(p/E)^{1/2}\right],$$

with

$$C = 2.92\times10^3\,\mathrm{m^{-1}\,Torr^{-1}},$$

$$D = 2.66\times10^2\,\mathrm{V^{1/2}(m\,Torr)^{-1/2}}$$

for argon and

$$C = 4.4\times10^2\,\mathrm{m^{-1}\,Torr^{-1}},$$

$$D = 1.4\times10^2\,\mathrm{V^{1/2}(m\,Torr)^{-1/2}}$$

for helium [8]. The rate coefficient of dissociative recombination was set equal to $5.38\times10^{-14}\,\mathrm{m^3s^{-1}}$ for argon [9] and $3.75\times10^{-17}\,\mathrm{m^3s^{-1}}$ for helium [10]. Electron mobility was estimated using the formulas $\mu_e = 10^{24}/n_n\,\mathrm{m^{-1}V^{-1}s^{-1}}$ for argon and $\mu_e = 2.25\times10^{24}/n_n\,\mathrm{m^{-1}V^{-1}s^{-1}}$ for helium (n_n is the density of the neutral gas), which represent an approximation of mobility data calculated using Bolsig+ [11]. Mobility of ions is estimated by means

of the formulas $\mu_i = 7.1\times10^{21}/n_n \mathrm{m}^{-1}\mathrm{V}^{-1}\mathrm{s}^{-1}$ for argon and $\mu_i = 5.5\times10^{22}/n_n \mathrm{m}^{-1}\mathrm{V}^{-1}\mathrm{s}^{-1}$ for helium, which are an approximation of measurements [12]. The diffusion coefficients of the ions and the electrons were evaluated with the use of Einstein's relation with the gas and electron temperatures equal to 300K and 1eV, respectively.

The detailed model takes into account atomic ions, molecular ions, electrons, atoms in excited states, excimers, and comprises conservation equations for all species, transport equations for all species written in the drift-diffusion approximation for the charged species and in the form of Fick's law for excited atoms and excimers, the Poisson equation, and the equation of conservation of electron energy which is written in the form recommended in [11]:

$$\nabla\cdot\mathbf{J}_{i1} = S_{i1}, \quad \mathbf{J}_{i1} = -D_{i1}\nabla n_{i1} - n_{i1}\mu_{i1}\nabla\varphi,$$

$$\nabla\cdot\mathbf{J}_{i2} = S_{i2}, \quad \mathbf{J}_{i2} = -D_{i2}\nabla n_{i2} - n_{i2}\mu_{i2}\nabla\varphi,$$

$$\nabla\cdot\mathbf{J}_{e} = S_{e}, \quad \mathbf{J}_{e} = -D_{e}\nabla n_{e} + n_{e}\mu_{e}\nabla\varphi,$$

$$\nabla\cdot\mathbf{J}_{M1} = S_{M1}, \quad \mathbf{J}_{M1} = -D_{M1}\nabla n_{M1},$$

$$\nabla\cdot\mathbf{J}_{M2} = S_{M2}, \quad \mathbf{J}_{M2} = -D_{M2}\nabla n_{M2},$$

$$\varepsilon_0\nabla^2\varphi = -e\left[n_{i1} + n_{i2} - n_e\right],$$

$$\nabla\cdot\mathbf{J}_{\varepsilon} = F_{\varepsilon} - S_{\varepsilon}, \quad \mathbf{J}_{\varepsilon} = -D_{\varepsilon}\nabla n_{\varepsilon} + n_{\varepsilon}\mu_{\varepsilon}\nabla\varphi.$$

Here the indexes *i1*, *i2*, *e*, *M1*, *M2* and ε refer to atomic ions, molecular ions, electrons, atoms in excited states, excimers, and average electron energy, respectively; n_α is number density of species α; the electron energy density is defined as $n_\varepsilon = n_e\bar{\varepsilon}$, where $\bar{\varepsilon}$ is the average electron energy, and coincides to the accuracy of a factor of 2/3 with electron pressure; φ is electric potential; S_α is the rate of production of particles of species α per unit time and unit volume; S_ε is the rate of loss of electron energy per unit time and unit volume due to collisions; $F_\varepsilon = -e\mathbf{J}_e\cdot\mathbf{E}$ is the rate of gain of electron energy per unit time and unit volume due to Joule heating; D_α is diffusion coefficient of species α in the gas of neutral atoms; D_ε is the so-called electron energy diffusion coefficient; μ_α is mobility of species α in the neutral gas of atoms; μ_ε is the so-called electron energy mobility.

The kinetic scheme is as follows. A single representative excited state for argon is considered which includes all excited states in the 4*s* manifold. Higher-order excited states are assumed to decay instantly into a level within the 4*s* manifold. Ionization channels taken into account are direct and stepwise ionization, metastable pooling, and ionization of excimers by electron impact. Conversion of atomic ions into molecular ions is taken into account, as well as spontaneous decay of excited atoms and excimers.

The electron kinetic and transport coefficients were calculated by means of Bolsig+ [11] using cross sections [13]. Rate coefficient of ionization from excited states in the 4*s* manifold was computed using formula of [14]. Rate coefficients for the other processes were taken from [15, 16].

A cylindrical discharge tube is considered, with bases of the cylinder being the electrodes and the lateral surface (wall) being insulating. Boundary conditions at the electrodes are written assuming that diffusion of the charged particles attracted by the electric field is negligible compared to drift. The boundary conditions at the wall are written under the assumption that all species coming to the wall are reflected.

3. Results and discussion

The formulated problem admits a 1D solution with all discharge parameters varying only in the axial direction. This is basically the classic von Engel and Steenbeck solution.

The current density voltage characteristics (CDVCs) described by this 1D solution referring to microdischarge in argon computed by means of the basic and detailed models are shown in figure 1 for the pressure of 30Torr and interelectrode gap *h* of 0.5mm. For comparison, also shown are the CDVC

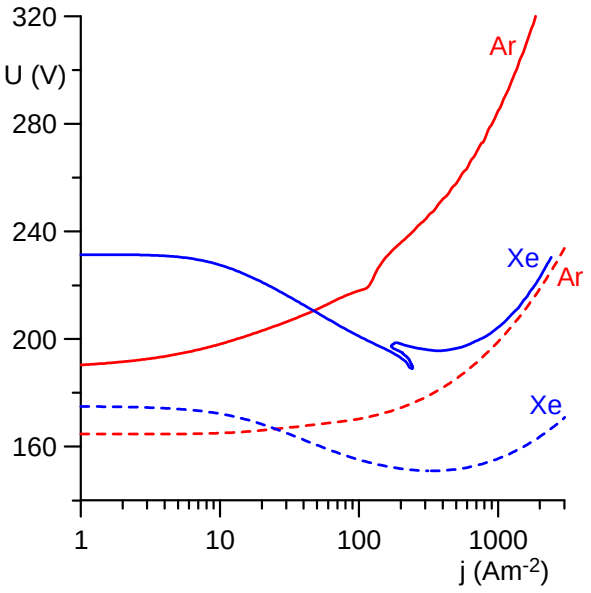

Figure 1: CDVCs of the 1D mode. p = 30Torr, h = 0.5mm. Solid: detailed model. Dashed: basic model.

described by the 1D mode for xenon under the same conditions, computed by means of the basic model [2] and a detailed model [7] which is similar to the above-described one for argon. For both argon and xenon, the CDVC obtained in the framework of the basic model is similar to the one obtained in the framework of the detailed model.

In addition to the 1D solution shown in figure 1, the considered problem may admit multidimensional solutions, describing self-organized spot patterns. In the case of xenon, the modelling in the framework of the basic model for the same pressure, the same interelectrode gap, and discharge radius R=0.5mm [2-4] has indeed revealed two 2D modes and thirteen 3D modes; at least three 2D modes exist under the same conditions in the framework of a similar detailed model for xenon [7]. Each of these multidimensional solutions branches off, or joins, the 1D solution shown in figure 1 at two states (bifurcation points), both positioned on the falling section of the CDVC.

In the case of argon, however, the CDVC has no falling section; a feature characteristic of an obstructed discharge. This suggests that there are no multidimensional modes bifurcating from the 1D mode in microdischarge in argon. It has been confirmed by bifurcation analysis performed as described in [17] in the framework of the basic model that the latter is indeed the case. These results represent a quite clear indication that conditions of argon microdischarges are not as favourable for the appearance of spot patterns as conditions of microdischarges in xenon.

The difference between CDVCs of the 1D mode for xenon and argon can be understood by comparing cross sections of elastic collisions between electrons and the atoms. These cross sections are shown in figure 2 for the values of average electron energy of interest. Also shown are cross sections of elastic collisions between electrons and helium atoms. The fact that the cross section of elastic collisions between electrons and atoms is larger for xenon than for argon is the reason why the discharge in argon is obstructed under the conditions considered: since the mean free path of electrons in argon is higher, the ionization coefficient of argon saturates at discharge currents lower than in xenon for the same product of pressure and interelectrode gap and the discharge in argon operates on the left-hand side of the Paschen curve. This effect should be even more pronounced for helium, since the corresponding cross sections are even lower than those of argon. (Note that the average electron energy in a helium glow discharge should be higher than in xenon and argon due to a higher ionization potential.)

If product of pressure and interelectrode gap is increased sufficiently, a falling section of the CDVC will appear. An illustration is given in figure 3. In this figure the calculated CDVC of the 1D mode in the framework of the basic model for argon is shown for a pressure of 75Torr and for the same interelectrode gap of 0.5mm. The pressure was chosen such that the falling section of the CDVC decreases by about 15% of the breakdown voltage, as it does in baseline calculations for xenon at a pressure of 30Torr and the same interelectrode gap of 0.5mm.

Also shown in figure 3 is a CDVC calculated for helium in the framework of the basic model for the same interelectrode gap. The pressure is set equal to 530Torr; a falling section of the CDVC is present for this pressure with a decrease of about 15% of the breakdown voltage.

Bifurcation analysis has shown that at least five multidimensional modes exist for each plasma-producing gas (argon and helium) under conditions of figure 3. Bifurcation points where the first and second 3D modes (the one with a spot at the periphery and the one with two spots at the periphery opposite each other) branch off, or join, the 1D mode are shown in figure 3. One can see that modes with spot patterns do occur in plasma-producing gases other than xenon provided that the conditions are right.

The above-mentioned calculations were performed neglecting neutralization of the charged

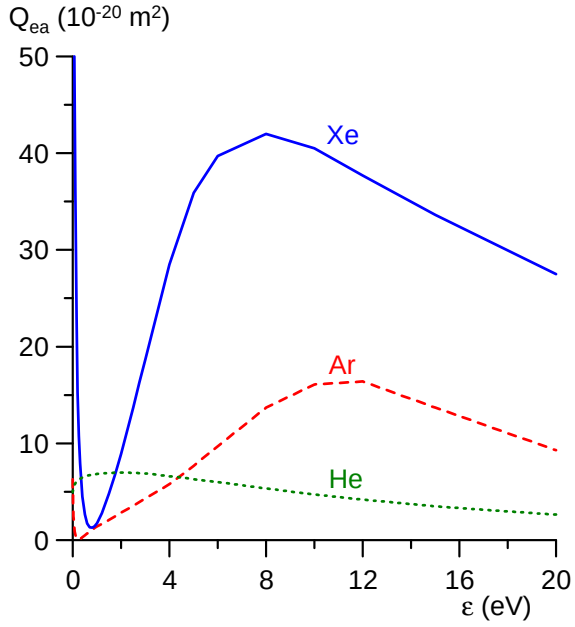

Figure 2: Cross sections of elastic collisions between electrons and neutrals as a function of electron energy.

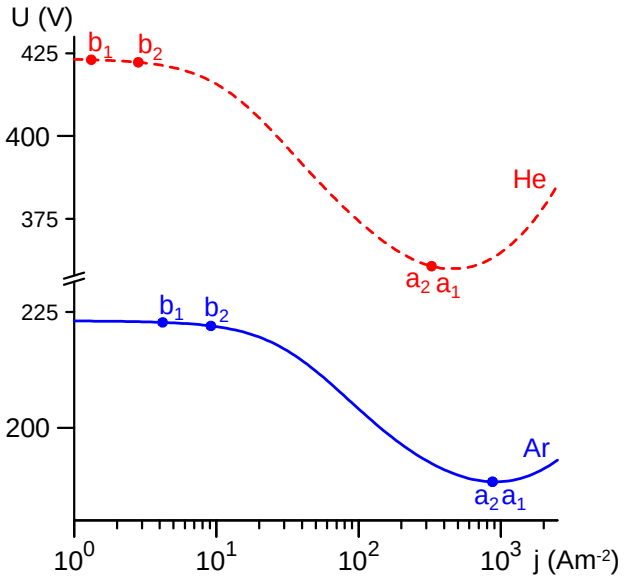

Figure 3: CDVCs of the 1D mode. h = 0.5mm, basic model. Solid: argon, p = 75Torr: Dashed: helium, p = 530Torr. Circles: bifurcation points of the first (a1, b1) and second (a2, b2) 3D modes for R = 0.5mm.

particles at the lateral wall of the discharge vessel. When neutralization of charged species at the wall is taken into account, a diffusion flux will appear in radial direction, which tends to smooth out perturbations, in accordance with numerical results reported in [2]. Increased values of diffusion coefficients in argon and helium enhance this stabilizing effect. Therefore, the effect of reduction of the number of non-fundamental modes when neutralization at the wall is taken into account should be more significant in argon than in xenon and even more significant in helium. In accordance with results in [2], the effect of increase of diffusion coefficients can be compensated by means of an increase of the radius of the discharge vessel.

4. Conclusions

Numerical results for argon, obtained in the framework of the detailed and basic models, and those for helium, obtained in the framework of the basic model, give a clear indication that the conditions of argon and helium microdischarges are less favourable for self-organization than those in xenon. This is a consequence of the difference between cross sections of elastic collisions between electrons and atoms of these gases. However, it should be possible to observe self-organization also in argon and helium microdischarges provided that the pressure is sufficiently high and the discharge radius is sufficiently large. It would be interesting to try to observe self-organization in experiments with argon microdischarges with a larger radius and higher pressure than in [6].

5. Acknowledgments

This work was performed within activities of the project PTDC/FIS/68609/2006 of FCT, POCI 2010 and FEDER and of the project Centro de Ciências Matemáticas of FCT, POCTI-219 and FEDER. P. G. C. Almeida and M. J. Faria appreciate PhD fellowships from FCT, grants SFRH/BD/30598/2006 and SFRH/BD/35883/2007.

5. References

[1] K. H. Schoenbach, M. Moselhy, and W. Shi, Plasma Sources Sci. Technol. 13 (2004) 177.

[2] P. G. C. Almeida, M. S. Benilov, and M. J. Faria, Plasma Sources Sci. Technol. 19 (2010) 025019.

[3] P. G. C. Almeida, M. S. Benilov and M. J. Faria, IEEE Trans. Plasma Sci. 39 (2011) to appear.

[4] P. G. C. Almeida, M. S. Benilov, M D Cunha and M. J. Faria, J. Phys. D: Appl. Phys. 42 (2009) 194010.

[5] M. S. Benilov, Sov. Phys. - Tech. Phys. 33 (1988) 1267.

[6] M. Moselhy, I. Petzenhauser, K. Frank, and K. H. Schoenbach, J. Phys. D: Appl. Phys. 36 (2003) 2922.

[7] P. G. C. Almeida, *Investigation of modes of current transfer in DC glow and arc discharges*, PhD thesis, Universidade da Madeira (2011).

[8] Yu. P. Raizer, *Gas Discharge Physics* (Springer, Berlin, 1991).

[9] A. N. Bhoj and M. J. Kushner, J. Phys. D: Appl. Phys. 37 (2004) 2510.

[10] Y. Sakiyama and D. B. Graves, J. Phys. D: Appl. Phys. 39 (2006) 3451.

[11] G. J. M. Hagelaar and L. C. Pitchford, Plasma Sources Sci. Technol. 14 (2005) 722.

[12] M. A. Biondi and L. M. Chanin, Phys. Rev. 94 (1954) 910.

[13] M. Hayashi, NIFS - Data 72 (2003).

[14] L. Vriens and A. H. M. Smeets, Phys. Rev. A 22 (1980) 940.

[15] G. M. Petrov and C. M. Ferreira, Private communication (2010).

[16] A. N. Bhoj and M. J. Kushner, J. Phys. D: Appl. Phys. 37 (2004) 2510.

[17] M. J. Faria, *Stability and bifurcations of modes of current transfer to cathodes of DC gas discharges*, PhD thesis, Universidade da Madeira (2011).